JOURNAL OF MATERIALS SCIENCE 6 (1971) 582–596

Study of Molecular Motion in Drawn Polyethylene by Broad-Line Nuclear Magnetic Resonance

M. J. FOLKES,
H. H. Wills Physics Laboratory, University of Bristol, UK

I. M. WARD
Department of Physics, University of Leeds, UK

Measurements have been made of the anisotropy in the nuclear magnetic resonance second moment for the proton resonance in drawn low density polyethylene films over the temperature range − 196 to + 60°C.

The experimental results are first compared with the theoretical predictions of a model in which it is assumed that the polyethylene chains undergo coherent classical rotation about the chain axis. This model is successful in predicting the general pattern of anisotropy at temperatures close to the melting point.

To account for the observed reduction in second moment at intermediate temperatures further calculations are described, based on a model in which the polyethylene chains twist about the chain axis, the total twist being shared equally between all monomer units. This does not account satisfactorily for the changes in second moment with temperature.

It is concluded that satisfactory general agreement between theory and experiment is reached if the measured anisotropy at intermediate temperatures derives from rigid lattice intramolecular interactions only, and that the intermolecular interactions are averaged to a small value. It is suggested that the inter-chain averaging occurs by a chain-sliding process.

At higher temperatures further reduction in the second moment occurs due to coherent chain oscillation about the chain axis, which finally leads to complete rotation at pre-melting point temperatures.

1. Introduction

During the last few years fairly extensive research has been carried out on broad line nuclear magnetic resonance studies of drawn polymers. Much of the work has produced interesting qualitative information concerning the origin of the anisotropy in the nuclear magnetic resonance second moment (see, for example, [1, 2]).

Recently McBrierty and Ward [3] reported measurements of the anisotropy of the rigid lattice NMR second moment on uniaxially cold-drawn low density and linear polyethylene. It was shown that the observed anisotropy could be related to the degree of molecular orientation of the drawn sample by development of the Van Vleck second moment formula [4].

Measurements of the anisotropy enable the orientation of the drawn polymer to be characterised to a good degree of accuracy in terms of orientation functions involving the second and fourth Legendre polynomials.

These orientation functions were then used to predict the anisotropy of the mechanical properties. They also serve the purpose of defining the orientation of the drawn polymer for studies of molecular motion.

The study of molecular motion in drawn polymers is of considerable importance in understanding mechanical relaxations. In polyethyl-

ene, measurements of the elastic moduli and loss angle over a wide frequency/temperature range have shown the existence of several relaxation maxima (for review see [5]).

In this paper we will be concerned with a detailed discussion of the molecular interpretation of the γ relaxation only.

2. Experimental

2.1. Sample Preparation

The samples of low density polyethylene examined for this investigation were the same as previously used for measurements of the rigid lattice second moment anisotropy [3] and were prepared as follows. Sheets 0.05 cm thick were formed from Alkathene WNF–15 (melt flow index 7, density 0.917 gcm^{-3}) by compression moulding at 150°C and subsequent quenching in water at room temperature. Samples 10 × 10 cm were cut from these sheets and then cold drawn at a rate of 1.25 cm min^{-1}, without necking, to a number of draw ratios. For the measurements recorded in this paper a draw ratio of 3.7 was used.

Circular samples 0.9 cm in diameter, cut from the drawn sheet, were then stacked on the shaft of the NMR probe, care being taken to ensure that the draw direction of each sample was parallel to its neighbour within a very small angle.

2.2. NMR Spectrometer

All the NMR measurements were performed with a Varian DP60 dual purpose spectrometer operating at a proton resonance frequency of 60 MHz (with a magnetic field of approximately 14 kG). The Varian sample holder was replaced by a square section boron glass shaft on which the samples were mounted. The top of this shaft was attached to a small goniometer head, thus enabling the draw direction of the samples to be set at any angle to the applied field H.

Low temperatures were achieved, either by passing dry compressed air through a copper spiral immersed in liquid air and allowing the cold gas to pass into the probe, or by directly boiling off liquid air. The latter technique has the considerable advantage of supplying completely dry gas which overcomes many of the problems associated with icing up of the fine bore tubes used to extract the gas from the probe.

Temperatures above room temperature were obtained by passing compressed air over a Nichrome heater. For both low and high temperature work the temperature was measured by means of a small copper-constantan thermocouple pressed against the samples.

The modulation field used had a peak-to-peak amplitude of 0.38 gauss and a frequency of 40 Hz.

The RF power level was chosen to avoid saturation of the spectra and was therefore different for different sample temperatures.

2.3. Second-moment Measurements

The second moment of the resonance line is defined by the following equation:

$$\langle \Delta H^2 \rangle = \langle (H\text{-}H^*)^2 \rangle = \frac{\int_{-\infty}^{\infty} f(H)(H\text{-}H^*)^2 \, d(H\text{-}H^*)}{\int_{-\infty}^{\infty} f(H) \, d(H\text{-}H^*)}$$

where H is the external magnetic field and H^* its value at the centre of the resonance and f(H) the absorption intensity at a magnetic field H.

The NMR spectra were recorded as derivative traces due to the audio-frequency modulation of the main field H. Integrating the above expression by parts yields the equivalent equation in terms of f′(H) the derivative of the absorption intensity:

$$\langle \Delta H^2 \rangle = \tfrac{1}{3} \frac{\int_{-\infty}^{\infty} f'(H)(H\text{-}H^*)^3 \, d(H\text{-}H^*)}{\int_{-\infty}^{\infty} f'(H)(H\text{-}H^*) \, d(H\text{-}H^*)}$$

The second moment was calculated numerically, using a digital computer, by reading from the NMR trace values of the derivative absorption intensity at small intervals of field H.

Measurements were carried out at angles of $\gamma = 0°$, 45°, and 90° where γ is the angle between the sample draw direction and magnetic field direction, at temperatures of −196, −100, −40, 23 and 60°C.

3. Theory

The starting point for the theory concerning the effect of motion on the second moment of the proton resonance spectra is the Van Vleck second moment equation [4]. This relates the second moment to the spatial co-ordinates of the resonating nuclei:

$$\langle \Delta H^2 \rangle = \frac{G}{N} \sum_{j>k} r_{jk}^{-6} (3 \cos^2 \beta_{jk} - 1)^2$$

where $G = \frac{3}{2}I(I + 1)g^2\mu_n^2$, I is the nuclear spin number, g the nuclear g-factor, μ_n the nuclear magneton, N the number of non-equivalent magnetic nuclei, r_{jk} the length of the vector joining nuclei j and k, and β_{jk} the angle between r_{jk} and the direction of the magnetic field.

The theory will be presented in two parts, one part concerned with the effect of motion on the intramolecular second moment, the other its effect on the intermolecular interactions.

In the previous paper the interpretation of the anisotropy in the second moment was made along the following lines. The partially oriented polymer can be considered to consist of an aggregate of anisotropic units of struture. Birefringence, X-ray diffraction and mechanical measurements have shown that the uniaxially cold-drawn sheets of low density polyethylene are transversely isotropic. The transverse isotropy was assumed to arise as follows. Firstly, the units of structure are transversely isotropic. Secondly, there is no preferential orientation of the units of structure in a plane perpendicular to the draw direction. To satisfy the first condition it was assumed that the units of structure consist of a number of unit cells of polyethylene, and that the symmetry axis of these units coincide with the c-axis of the polyethylene unit cells where the a and b axes are randomly oriented in the plane perpendicular to the symmetry axes.

This simple single phase model provided a qualitative interpretation of the NMR anisotropy, but did not give a satisfactory prediction of the optical and mechanical anisotropy. It was therefore decided to adopt a two phase model of crystalline and amorphous regions and to assume that from the NMR viewpoint the amorphous phase can be considered isotropic. With this assumption the NMR anisotropy relates to the orientation of the crystalline regions only, and can be used to calculate the corresponding orientation functions. A good fit to the optical and mechanical anisotropy was then obtained.

In this paper we will be concerned with the NMR anisotropy of the crystalline regions. As the measurements were undertaken under conditions where a composite signal was observed the second moment of the crystalline region could be determined separately, if we make the assumption that the broad component arises only from these regions.

It was emphasised in the previous publication that the interpretation of the NMR anisotropy relies on the validity of a formal mathematical argument and should not be taken to imply that there exist unique units of structure of the type described in the model. The interpretation certainly suggests that the NMR anisotropy arises from the crystalline regions of the polymer, but we have no information regarding the size and shape of the crystalline regions. We do know that the calculated NMR anisotropy relates to proton interactions within a sphere of radius 5 Å in the crystalline regions, and that this gives values for the rigid lattice second moments which are close to those observed.

3.1. Effect of Motion on the Intramolecular Second Moment

We will now consider the effect on the second moment of a coherent classical rotation of the polyethylene chains about the chain axes (coincident with the c-axis of the orthorhombic unit cell of polyethylene). By coherent, is meant a chain is regarded as rotating as a complete

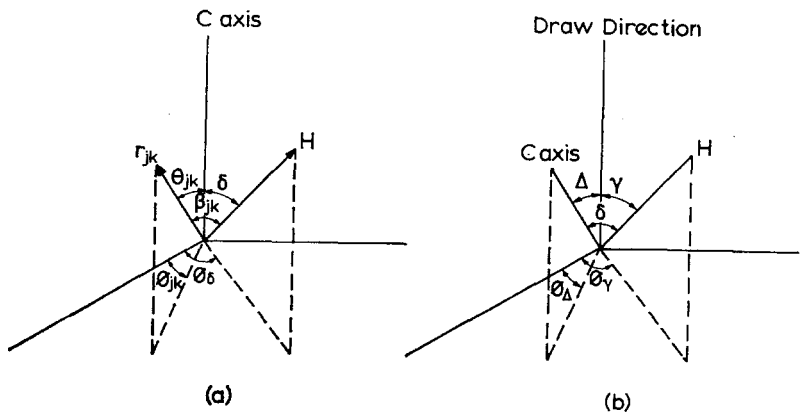

Figure 1 Notation used in the calculation of the effect of motion on the second moment.

entity without change in the interproton distances within that chain.

The principal stages in the calculation are as follows. With reference to fig. 1 we first consider a particular internuclear vector $\mathbf{r}_{jk}$ which makes an angle β_{jk} with the external field H. In the previous calculation for the rigid lattice situation [3] the factor $(3\cos^2\beta_{jk} - 1)^2$ was averaged by first relating β_{jk} to the intermediate angles θ_{jk}, ϕ_{jk}, δ and ϕ_δ and subsequently averaging the azimuthal angle ϕ_{jk} over the range $0 \leqslant \phi_{jk} \leqslant 2\pi$. This step was based on the assumption of transverse isotropy of the internuclear vectors about the c-axis of the unit of structure. In the case of motion of the internuclear vectors $\mathbf{r}_{jk}$ about the c-axis it can be shown that it is the factor $(3\cos^2\beta_{jk} - 1)$ which must be averaged (see for example, [6]) and the result of this averaging is then squared.

Summarising then, the basic difference between the rigid lattice and motion calculations is that in the former the assumption of transverse isotropy of the internuclear vectors $\mathbf{r}_{jk}$ about the c-axis implies that we must evaluate

$$\langle(3\cos^2\beta_{jk} - 1)^2\rangle_{Av\phi_{jk}}$$

whereas for the situation in which the internuclear vectors are in motion about the c-axis we evaluate

$$(\langle(3\cos^2\beta_{jk} - 1)\rangle_{Av\phi_{jk}})^2.$$

The second part of the calculation of the effect of motion on the second moment will involve relating the angle δ to the angles Δ, ϕ_Δ, γ and ϕ_γ which define the angle between the c-axis of the unit of structure and the magnetic field H and its relationship to the draw direction of the sample. In this case we take a "fibre average", which means we assume we have transverse isotropy of the units of structure about the draw direction, that is, we average ϕ_Δ over the range $0 \leqslant \phi_\Delta \leqslant 2\pi$.

It is proposed to present the calculation in terms of Euler angle transformations, but for completeness the treatment using spherical harmonic analysis is given in the Appendix. The Euler angle method is particularly convenient for the calculation of the effect of motion on the intermolecular interactions which is also carried out later in the paper.

By the Van Vleck equation:

$$\langle\Delta H^2\rangle = \frac{G}{N}\sum_{j>k}\left\{\frac{3\cos^2\beta_{jk} - 1}{r_{jk}^3}\right\}^2$$

and since the interproton distances remain fixed throughout the motion we will only need to transform the numerator of this expression.

We may relate β_{jk} to the intermediate angles θ_{jk} and δ by:

$$\cos\beta_{jk} = \cos\theta_{jk}\cos\delta + \sin\theta_{jk}\sin\delta\cos(\phi_\delta - \phi_{jk})$$

so that

$$\begin{aligned}(3\cos^2\beta_{jk} - 1) &= 3\{\cos\theta_{jk}\cos\delta + \sin\theta_{jk}\sin\delta\cos(\phi_\delta - \phi_{jk})\}^2 - 1 \\ &= 3\cos^2\theta_{jk}\cos^2\delta + 6\cos\theta_{jk}\sin\theta_{jk}\cos\delta\sin\delta\cos(\phi_\delta - \phi_{jk}) \\ &\quad + 3\sin^2\theta_{jk}\sin^2\delta\cos^2(\phi_\delta - \phi_{jk}) - 1\end{aligned}$$

For rotation of the chain about the c-axis we calculate:

$$\begin{aligned}\langle(3\cos^2\beta_{jk} - 1)\rangle_{Av\phi_{jk}} &= 3\cos^2\theta_{jk}\cos^2\delta \\ &\quad + \tfrac{3}{2}\sin 2\theta_{jk}\sin 2\delta\,\overline{\cos(\phi_\delta - \phi_{jk})} \\ &\quad + 3\sin^2\theta_{jk}\sin^2\delta\,\overline{\cos^2(\phi_\delta - \phi_{jk})} - 1\end{aligned}$$

where we average ϕ_{jk} over all angles between 0 and 2π with a uniform probability function, so that:

$$\overline{\cos(\phi_\delta - \phi_{jk})} = \frac{1}{2\pi}\int_0^{2\pi}\cos(\phi_\delta - \phi_{jk})\,d\phi_{jk} = 0$$

and

$$\overline{\cos^2(\phi_\delta - \phi_{jk})}\,\frac{1}{2\pi}\int_0^{2\pi}\cos^2(\phi_\delta - \phi_{jk})\,d\phi_{jk} = \tfrac{1}{2}.$$

Hence

$$\begin{aligned}\langle 3\cos^2\beta_{jk} - 1\rangle_{Av\phi_{jk}} &= 3\cos^2\theta_{jk}\cos^2\delta + \tfrac{3}{2}\sin^2\theta_{jk}\sin^2\delta - 1 \\ &= \tfrac{1}{2}(3\cos^2\theta_{jk} - 1)(3\cos^2\delta - 1)\end{aligned}$$

This result must now be squared and averaged to give transverse isotropy for the c-axes of the units of structure about the draw direction.
Hence

$$(\langle 3\cos^2\beta_{jk} - 1\rangle_{Av\phi_{jk}})^2 = \tfrac{1}{4}(3\cos^2\theta_{jk} - 1)^2(3\cos^2\delta - 1)^2$$

and we now relate the angle δ to the intermediate angles Δ and γ by the Euler transformation:

$$\cos\delta = \cos\Delta\cos\gamma + \sin\Delta\sin\gamma\cos(\phi_\gamma - \phi_\Delta)$$

so that:

$$\begin{aligned}(3\cos^2\delta - 1)^2 &= [3\{\cos\Delta\cos\gamma + \sin\Delta\sin\gamma\cos(\phi_\gamma - \phi_\Delta)\}^2 - 1]^2 \\ &= 9\{\cos\Delta\cos\gamma + \sin\Delta\sin\gamma\cos(\phi_\gamma - \phi_\Delta)\}^4 - 6\{\cos\Delta\cos\gamma \\ &\quad + \sin\Delta\sin\gamma\cos(\phi_\gamma - \phi_\Delta)\}^2 + 1\end{aligned}$$

This expression is expanded and since we require $\langle(3\cos^2\delta - 1)^2\rangle_{Av\phi_\Delta}$ to account for the transverse isotropy of the c-axis about the draw direction we can simplify the resulting expansion using the additional results:

$$\overline{\cos(\phi_\gamma - \phi_\Delta)} = 0 \qquad \overline{\cos^3(\phi_\gamma - \phi_\Delta)} = 0$$
$$\overline{\cos^2(\phi_\gamma - \phi_\Delta)} = \tfrac{1}{2} \qquad \overline{\cos^4(\phi_\gamma - \phi_\Delta)} = \tfrac{3}{8}$$

where these have been averaged over ϕ_Δ in the range $0 \leqslant \phi_\Delta \leqslant 2\pi$.

This averaging leads to the result:

$$\langle(3\cos^2\delta - 1)^2\rangle_{Av\phi_\Delta} = \tfrac{1}{8}\{(11 - 30\cos^2\gamma + 27\cos^4\gamma) + \overline{\cos^2\Delta}(252\cos^2\gamma - 270\cos^4\gamma - 30) + \overline{\cos^4\Delta}(315\cos^4\gamma - 270\cos^2\gamma + 27)\}$$

where $\overline{\cos^2\Delta}$ and $\overline{\cos^4\Delta}$ are the orientation functions describing the distribution of the units of structure about the draw direction.

This expression can now be substituted into the Van Vleck equation to give:

$$\langle\Delta H^2\rangle = \frac{G}{32N}\sum_{j>k} r_{jk}^{-6}(3\cos^2\theta_{jk} - 1)^2 \{(11 - 30\cos^2\gamma + 27\cos^4\gamma) + \overline{\cos^2\Delta}(252\cos^2\gamma - 270\cos^4\gamma - 30) + \overline{\cos^4\Delta}(315\cos^4\gamma - 270\cos^2\gamma + 27)\}$$

This is the modified Van Vleck equation for a transversely isotropic aggregate and a classical rotation of the molecular chains about the chain axes.

Clearly, if we use the appropriate values of $\overline{\cos^2\Delta}$ and $\overline{\cos^4\Delta}$ for a draw ratio of 3.7, as determined by McBrierty and Ward [3] from their rigid lattice second moment data, we can calculate the variation of $\langle\Delta H^2\rangle$ with orientation angle γ providing we also calculate the lattice sum:

$$S = \sum_{j>k} r_{jk}^{-6}(3\cos^2\theta_{jk} - 1)^2$$

This was calculated from a knowledge of the co-ordinates of the protons in a polyethylene chain using an Elliott 503 computer. The value was computed as $S = 0.0654$. It is of interest to note that the motional second moment depends on the value of only one lattice sum, whereas the rigid lattice second moment is dependent on three.

The predicted variation of the second moment with orientation angle for the intramolecular interactions is shown in fig. 2. We cannot make any realistic comparison, at this stage, between the theoretical and experimental results since we have ignored the proton interactions between chains. The intermolecular interactions in the rigid lattice situation are highly anisotropic and in fact result in the value of the second moment at $\gamma = 90°$ being larger than at $\gamma = 0°$. It is therefore necessary to perform a calculation of the intermolecular interactions in the case where there is chain rotation.

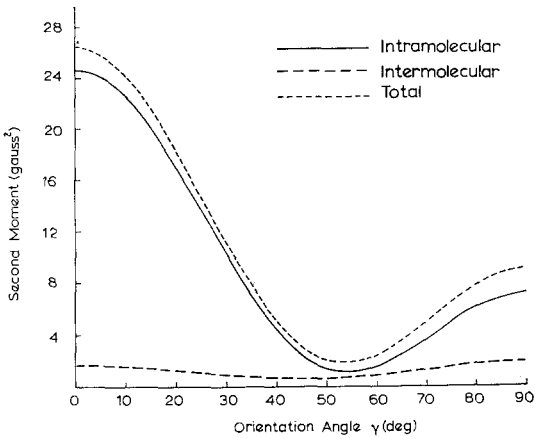

Figure 2 Predicted variation of the second moment for low density polyethylene – draw ratio 3.7, based on the coherent classical rotation model.

3.2. Effect of Motion on the Intermolecular Second Moment

The calculation of the effect of motion on the intermolecular second moment is related to the work of Andrew [7] on molecular motion in paraffins. Fig. 3 shows a diagram (to scale) of the a-b plane of a polyethylene unit cell with

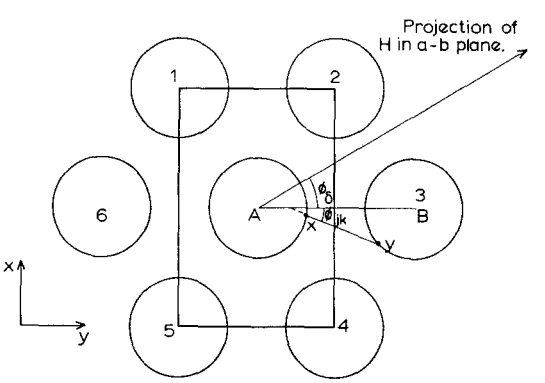

Figure 3 Projection in the a-b plane of a polyethylene unit cell. The circles represent the locus of the protons when the chains rotate about the c-axis.

molecular chains at the normal cell positions. When the chains undergo classical rotation about the *c*-axis it can be calculated from bond angles and lengths that the protons will sweep out a circle of radius 1.39 Å. The diagram only includes those chains whose protons will be at a distance of less than 5 Å at the closest distance of approach, with the protons belonging to the chain at the cell centre. We will assume that distances greater than 5 Å may be ignored. Due to the dependence of the second moment on the inverse sixth power of the distance between the protons this is a reasonable approximation.

An interesting fact now arises just from consideration of the geometry of fig. 3. The chains 1 to 6 and the one labelled "A" at the cell centre cannot move as a "set of meshed gear wheels" which would seem to be necessary, bearing in mind that the Van der Waals' diameter for protons is approximately 2.4 Å. This leads to two possible conclusions:

(i) Free uncorrelated chain rotation will occur only when lattice expansion is sufficiently great for these Van der Waal's interactions to be unimportant. Actually, even at room temperature, the lattice constants *a* and *b* are still not large enough to permit this. X-ray evidence, however, shows that as the temperature increases a gradual change from orthorhombic to hexagonal symmetry occurs. This effect is not entirely attributable to lattice expansion and the formation of a lattice of higher symmetry probably results from, at least, some chain rotation.

(ii) If uncorrelated chain rotation is energetically unfavourable then the chains can move in only a small number of alternative ways. The possibilities are chain twisting, coherent chain oscillation and a diffusion of chain segments past each other. The latter mechanism of chain sliding is similar to the γ_c relaxation proposed by Hoffman, Williams, and Passaglia [8].

The relevance of this to the experimental observations will be discussed in due course but for the moment, however, we will assume that uncorrelated chain rotation occurs and that the chains are arranged on a hexagonal lattice. This is a realistic approximation for polyethylene, and simplifies considerably the calculation of the intermolecular second moment since there is only one unique distance between chain centres for chain A and all of its nearest neighbours.

The major difference between the calculation of the intermolecular second moment and the intramolecular contribution is that in the latter the interproton distances remained constant whereas in the former we must begin by computing

$$\left\langle \left\{ \frac{3\cos^2\beta_{jk} - 1}{r_{jk}^3} \right\} \right\rangle$$

for the particular motion we envisage, i.e. r_{jk} for the intermolecular calculation is changing at all points of the motion and we must include this in our calculation.

Referring to figs. 1 and 3 we may write as before:

$$\cos\beta_{jk} = \cos\theta_{jk}\cos\delta + \sin\theta_{jk}\sin\delta\cos(\phi_\delta - \phi_{jk})$$

$$\therefore \left\{ \frac{3\cos^2\beta_{jk} - 1}{r_{jk}^3} \right\} = \frac{3\{\cos\theta_{jk}\cos\delta + \sin\theta_{jk}\sin\delta\cos(\phi_\delta - \phi_{jk})\}^2 - 1}{r_{jk}^3}$$

$$= \frac{3\cos^2\theta_{jk}\cos^2\delta + 6\cos\theta_{jk}\sin\theta_{jk}\cos\delta\sin\delta\cos(\phi_\delta - \phi_{jk})}{r_{jk}^3} + \frac{3\sin^2\theta_{jk}\sin^2\delta\cos^2(\phi_\delta - \phi_{jk}) - 1}{r_{jk}^3}.$$

$$\therefore \left\langle \left\{ \frac{3\cos^2\beta_{jk} - 1}{r_{jk}^3} \right\} \right\rangle = 3\cos^2\delta \left\{ \frac{\cos^2\theta_{jk}}{r_{jk}^3} \right\}_{Av} + \sin 2\delta \left\{ \frac{\frac{3}{2}\sin 2\theta_{jk}\cos(\phi_\delta - \phi_{jk})}{r_{jk}^3} \right\}_{Av}$$

$$+ \sin^2\delta \left\{ \frac{\frac{3}{2}\sin^2\theta_{jk}[1 + \cos 2(\phi_\delta - \phi_{jk})]}{r_{jk}^3} \right\}_{Av} - \left\{ \frac{1}{r_{jk}^3} \right\}_{Av} = 3\cos^2\delta \left\{ \frac{\cos^2\theta_{jk}}{r_{jk}^3} \right\}_{Av}$$

$$+ \tfrac{3}{2}\sin 2\delta\cos\phi_\delta \left\{ \frac{\sin 2\theta_{jk}\cos\phi_{jk}}{r_{jk}^3} \right\}_{Av} + \tfrac{3}{2}\sin 2\delta\sin\phi_\delta \left\{ \frac{\sin 2\theta_{jk}\sin\phi_{jk}}{r_{jk}^3} \right\}_{Av}$$

$$+ \tfrac{3}{2}\sin^2\delta \left\{ \frac{\sin^2\theta_{jk}}{r_{jk}^3} \right\}_{Av} + \tfrac{3}{2}\sin^2\delta\cos 2\phi_\delta \left\{ \frac{\sin^2\theta_{jk}\cos 2\phi_{jk}}{r_{jk}^3} \right\}_{Av}$$

$$+ \tfrac{3}{2}\sin^2\delta\sin 2\phi_\delta \left\{ \frac{\sin^2\theta_{jk}\sin 2\phi_{jk}}{r_{jk}^3} \right\}_{Av} - \left\{ \frac{1}{r_{jk}^3} \right\}_{Av}$$

and we may rewrite this in the more compact form:

$$\left\langle\left\{\frac{3\cos^2\beta_{jk}-1}{r_{jk}^3}\right\}\right\rangle = 3A\cos^2\delta + \tfrac{3}{2}B\sin 2\delta\cos\phi_\delta + \tfrac{3}{2}C\sin 2\delta\sin\phi_\delta + \tfrac{3}{2}D\sin^2\delta + \tfrac{3}{2}E\sin^2\delta\cos 2\phi_\delta + \tfrac{3}{2}F\sin^2\delta\sin 2\phi_\delta - G$$

where we have defined the following quantities to be averaged over θ_{jk}, ϕ_{jk} and r_{jk}:

$$A = \left\{\frac{\cos^2\theta_{jk}}{r_{jk}^3}\right\}_{Av}$$

$$B = \left\{\frac{\sin 2\theta_{jk}\cos\phi_{jk}}{r_{jk}^3}\right\}_{Av}$$

$$C = \left\{\frac{\sin 2\theta_{jk}\sin\phi_{jk}}{r_{jk}^3}\right\}_{Av}$$

$$D = \left\{\frac{\sin^2\theta_{jk}}{r_{jk}^3}\right\}_{Av}$$

$$E = \left\{\frac{\sin^2\theta_{jk}\cos 2\phi_{jk}}{r_{jk}^3}\right\}_{Av}$$

$$F = \left\{\frac{\sin^2\theta_{jk}\sin 2\phi_{jk}}{r_{jk}^3}\right\}_{Av}$$

$$G = \left\{\frac{1}{r_{jk}^3}\right\}_{Av}$$

The evaluation of these lattice sums will be described in more detail later, but a number of points can be made at this stage. First the sums must be averaged over θ_{jk} and ϕ_{jk} for the motion and they must be computed for all non-equivalent interactions between chains within the unit of structure up to a distance of 5 Å, i.e. we compute

$$A = \sum_{j>k}\left\{\frac{\cos^2\theta_{jk}}{r_{jk}^3}\right\}_{Av}$$

and similarly for the other lattice sums.

Fortunately in the model chosen there is only one unique interaction to be computed, but extending the calculation to include other interactions presents no problems. It should also be noted that only when ϕ_{jk} is averaged over the range 0 to 2π as in the case of the intra molecular interaction, do we obtain the simple result:

$$\langle 3\cos^2\beta_{jk}-1\rangle_{Av\phi_{jk}} = \tfrac{1}{2}(3\cos^2\theta_{jk}-1)(3\cos^2\delta-1)$$

In the more general case which is now being treated, the value of this average will depend on all of the lattice sums listed above.

For convenience we will put

$$\left\{\frac{3\cos^2\beta_{jk}-1}{r_{jk}^3}\right\} = y\,.$$

We require to find $(\bar{y})^2$. In the absence of any simplifying assumptions the resulting expression for $(\bar{y})^2$ will be extremely tedious to evaluate. Because the contribution to the second moment due to intermolecular interactions is much smaller than that due to intramolecular interactions, we are justified in introducing an approximation. This is to assume coplanar motion of the protons in neighbouring chains, i.e. $\theta_{jk} = 90°$. Non coplanar motions could also be readily considered by retaining the full expression for $\bar{y}$. We now have:

$$A = B = C = 0\,;\quad D = G = \left\{\frac{1}{r_{jk}^3}\right\}_{Av}$$

$$E = \left\{\frac{\cos 2\phi_{jk}}{r_{jk}^3}\right\}_{Av}$$

$$F = \left\{\frac{\sin 2\phi_{jk}}{r_{jk}^3}\right\}_{Av}$$

Hence

$$\bar{y} = \tfrac{3}{2}\sin^2\delta\{E\cos 2\phi_\delta + F\sin 2\phi_\delta + G\} - G$$

Squaring this and grouping terms gives the result:

$$(\bar{y})^2 = \tfrac{9}{4}\sin^4\delta\{E^2\cos^2 2\phi_\delta + F^2\sin^2 2\phi_\delta + EF\sin 4\phi_\delta + 2GE\cos 2\phi_\delta + 2FG\sin 2\phi_\delta + G^2\} - 3G\sin^2\delta\{E\cos 2\phi_\delta + F\sin 2\phi_\delta + G\} + G^2$$

Next it is assumed that there is transverse isotropy of the vectors joining chain A to all other neighbouring chains. Only under this condition can ϕ_δ be averaged over the range $0 \leqslant \phi_\delta \leqslant 2\pi$ and an expression for $(\bar{y})^2$ obtained which only involves δ. If we were to take a discrete average for $(\bar{y})^2$ over the chains 1 to 6 using the hexagonal symmetry about A we would still find that $(\bar{y})^2 = f(\delta, \phi_\delta)$.

Averaging ϕ_δ over 0 to 2π we have:

$$\overline{\cos^2 2\phi_\delta} = \overline{\sin^2 2\phi_\delta} = \tfrac{1}{2};\ \overline{\sin 2\phi_\delta} = \overline{\cos 2\phi_\delta} = \overline{\sin 4\phi_\delta} = 0$$

and hence:

$$(\bar{y})_{Av\phi_\delta} = \tfrac{9}{8}\sin^4\delta\{E^2 + F^2 + 2G^2\} - 3G^2\sin^2\delta + G^2$$

Following the lines of the intramolecular calculation the angle δ is related to the intermediate angles Δ, ϕ_Δ, γ and ϕ_γ by the Euler relation:

$$\cos\delta = \cos\Delta\cos\gamma + \sin\Delta\sin\gamma\cos(\phi_\gamma - \phi_\Delta)$$

This is now substituted into the above equation for $(\bar{y})^2_{Av\phi_\delta}$ and the resulting expression must be averaged over ϕ_Δ in the range 0 to 2π in accordance with the assumption of transverse isotropy of the c-axes of the units of structure about the draw direction. Carrying out this averaging leads to the following result:

$$\{(\bar{y})^2\}_{Av\phi_\delta,\phi_\Delta}$$
$$= \{3H - K + \cos^2\gamma\,(2H - 3K) + 3H\cos^4\gamma\}$$
$$+ \overline{\cos^2\Delta}\{2H - 3K + \cos^2\gamma\,(12H + 9K)$$
$$- 30H\cos^4\gamma\} + \overline{\cos^4\Delta}\{3H - 30H\cos^2\gamma$$
$$+ 35H\cos^4\gamma\}$$

where we have defined two new lattice sums:

$$H = \tfrac{9}{64}\{E^2 + F^2 + 2G^2\}\,; \quad K = \tfrac{1}{2}G^2\,.$$

Substituting this result into the Van Vleck equation gives:

$$\langle\Delta H^2\rangle_{INTER}$$
$$= \frac{G}{N}\sum_{j>k}[\{3H - K + \cos^2\gamma(2H - 3K)$$
$$+ 3H\cos^4\gamma\} + \overline{\cos^2\Delta}\{2H - 3K$$
$$+ \cos^2\gamma(12H + 9K) - 30H\cos^4\gamma\}$$
$$+ \overline{\cos^4\Delta}\{3H - 30H\cos^2\gamma + 35H\cos^4\gamma\}]$$

This is the modified Van Vleck equation for the intermolecular second moment for a coplanar system of rotating protons. In principle the problem is now solved, provided that the lattice sums E, F and G are evaluated. This involves averaging the interactions between pairs of rotating protons, whose motions are uncorrelated. This calculation has been carried out previously [7].

The final value of the lattice sums depends only on the distance between chain centres and the radius of the circular path swept out by the rotating protons. Using published values for the lattice constants at room temperature for low density polyethylene and the co-ordinates of the protons, the following values were obtained for E, F and G:

$$E = 0.03954;\ F = 0 \text{ (from symmetry of motion)}$$
$$G = 0.04582;$$

giving H = 0.001621, K = 0.002099

These values enable the variation of the intermolecular second moment with orientation angle γ to be determined if values of $\overline{\cos^2\Delta}$ and $\overline{\cos^4\Delta}$ are inserted into the equation. As before, these values are taken as the rigid lattice orientation functions as determined by McBrierty and Ward [3]. The predicted anisotropy of the intermolecular second moment is shown in fig. 2 together with the total second moment, which is just the algebraic sum of the intra and inter components. It is interesting that the intermolecular second moment is very small $\sim$ 1 to 2 gauss^2 when motional averaging occurs and the anisotropy in the second moment is also very small. This is to be contrasted with a rigid lattice intermolecular second moment $\sim$ 9 gauss^2.

4. Results and Discussion

4.1. General Features

Fig. 4 shows the first derivative of the NMR spectra obtained with cold drawn low density polyethylene at the temperature and alignment angles γ as indicated. On the simplest model, polyethylene can be regarded as consisting of two phases – a crystalline and amorphous phase and the proportion of each will depend on preparation conditions, draw ratio etc. The observed NMR spectra can then be regarded as the sum of the spectra that would be obtained separately from the crystalline and amorphous regions.

First, a simple qualitative interpretation will be given of the changes which occur with temperature. At low temperatures ($\sim$ – 196°C) any chain motion will be quenched and the material possesses a rigid structure. Since the predominant contribution to the line width of the NMR spectra will derive from proton interactions within a chain, it is to be expected that the NMR spectra from both the crystalline and amorphous phases will be approximately similar at these temperatures. This accounts for the presence of only a single broad component in the spectra and it is only at $\gamma = 90°$ that the narrow component is slightly visible.

As the temperature is raised, a narrow component is observed, which increases in amplitude with increasing temperature, being particularly noticeable at – 40°C and $\gamma = 0°$ in fig. 4. This effect is attributed to hindered rotation of the chain molecules, predominantly in the amorphous regions where interchain proton interactions are small.

Further increase in temperature results in a rapid decrease in the broad component of the spectra and at 23°C a two phase structure is clearly visible at $\gamma = 0°$. At 60°C liquid-like spectra are found in which nearly all the molecular chains are in motion in both the crystalline and

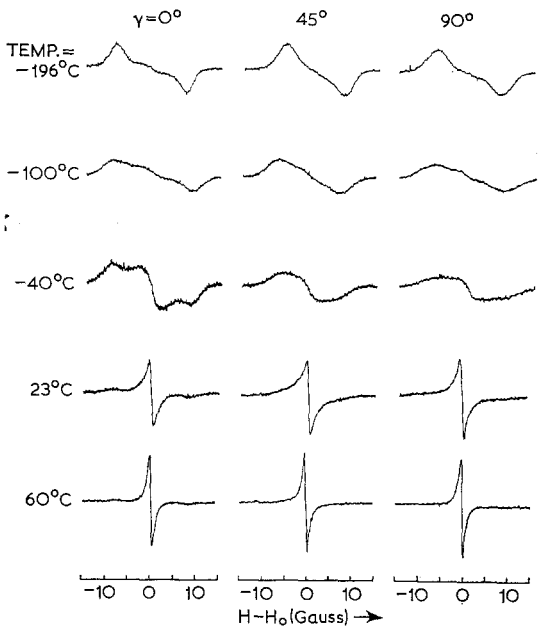

Figure 4 First derivative of the proton resonance absorption signal in cold drawn low density polyethylene–draw ratio 3.7, obtained at different orientation angles γ and sample temperatures.

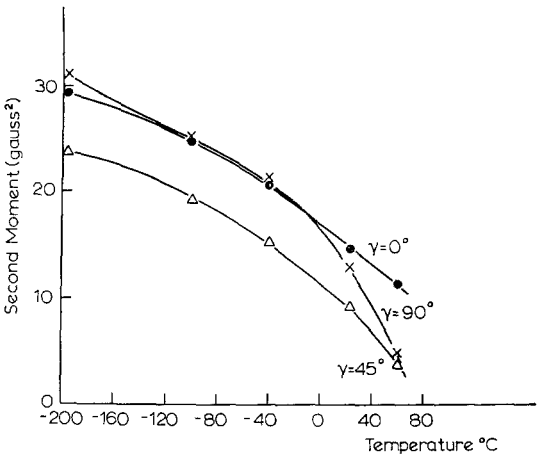

Figure 5 Experimental variation of the second moment with temperature for various orientations γ for cold drawn low density polyethylene – draw ratio 3.7.

amorphous phases. Further increase in temperature only results in a rapid melting of the specimens.

It is of interest at this stage to compare these results with those obtained by Olf and Peterlin [1] for high density linear polyethylene. Their measurements show very similar spectra at a temperature of − 196°C, but a two phase structure is only visible at around room temperature, as compared with − 40°C on our measurements. Even at 125°C a very clear two component curve is recorded in their case.

These differences can be attributed to the effect of branching on the molecular mobility in polyethylene. The presence of greater concentrations of branch points in the low density polyethylene compared with the high density polymer gives rise to a correspondingly greater degree of molecular mobility at a given temperature.

Apart from direct temperature differences just described, there are also significant detailed differences in the anisotropy of the spectra with the alignment angle γ although, as will be discussed later, the anisotropy of the second moment with angle γ is very similar for both Olf and Peterlin's [1] results and ours.

Fig. 5 shows the variation of the second moment with sample temperature at the three orientations $\gamma = 0°$, 45° and 90° of the draw direction with respect to the magnetic field H.

It should be noted that the minimum of the second moment occurs at $\gamma = 45°$ for all temperatures in the range − 196 to 60°C. In addition the maximum of the second moment is at $\gamma = 90°$ for temperatures less than − 15°C, but shifts to $\gamma = 0°$ for temperatures greater than this value.

4.2. Detailed Analysis of the Broad Component of the NMR Spectra

For two reasons, we have confined our attention to a discussion of the broad component only. First, the crystalline regions giving rise to the broad component are in a more defined state than the tangled amorphous regions. This enables us to use the results of our theoretical calculation in which we assumed the polyethylene chains occupied distinct positions on an orthorhombic lattice. Second, the previous paper on the anisotropy of the rigid lattice second moment enabled orientation functions to be evaluated, which defined the orientation of the crystalline regions of the sample. The NMR spectra were therefore decomposed into a broad and narrow component. Although this is a somewhat arbitrary process most of the uncertainty in constructing the broad line curve from the composite signal arises close to the peak of the absorption curve, and this region does not contribute greatly to the second moment.

Fig. 6 shows the variation of the second moment of the broad component with temperature for various orientations γ. It is interesting that the curves for $\gamma = 0°$ and 90° converge at a temperature of − 100°C.

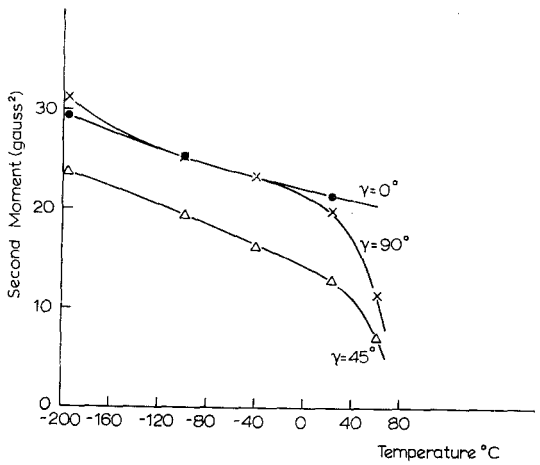

Figure 6 Experimental variation of the second moment of the broad component with temperature for various orientations γ for cold drawn low density polyethylene – draw ratio 3.7.

The anisotropy of the second moment with orientation angle γ for various temperatures is clearly seen in fig. 7. The second moment is seen to reduce with increasing temperature for $\gamma = 90°$. This is to be expected if the polyethylene chains are undergoing motion about the c-axis of the unit cell. A more surprising result is the reduction in the second moment with increasing temperature for $\gamma = 0°$. It can be seen that the effect is considerable – a reduction of ~ 9 gauss² from a temperature of − 196 to 60°C.

Before we compare our experimental results with those predicted on the basis of the coherent classical rotation model it is necessary once again to draw attention to the quite significant differences in the pattern of behaviour of second moment versus temperature for low-density and linear polyethylene.

The results we report for the variation of second moment as a function of temperature and orientation γ for low-density polyethylene closely follow results reported elsewhere, e.g. [9] and [10]. In all these cases it is apparent that the second moment, particularly for $\gamma = 0°$ and 90°, falls quite considerably over the range − 196 to about 20°C. This is to be compared with the results for linear polyethylene reported by Olf and Peterlin [1] in which the second moment for $\gamma = 0°$ and 90° exhibits only a slight decrease over this range.

4.2.1. Comparison of Experimental Results with a Classical Rotation Model

It is seen immediately when figs. 2 and 7 are compared that at no temperature is there agreement between the experimental and predicted curves based on a rotating chain model. However, the theoretical curve predicts a large anisotropy in second moment at $\gamma = 0°$ and 90° and it is this feature that is exhibited by the curve at 60°C shown in fig. 7. The absolute value

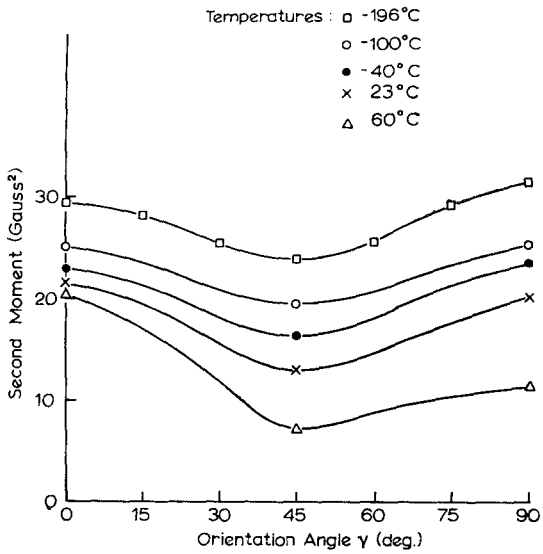

Figure 7 Experimental variation of the crystalline second moment with orientation angle γ for cold drawn low density polyethylene – draw ratio 3.7.

of the second moment for $\gamma = 0°$, is smaller than predicted in fig. 2, but this reduction is easily explained if the orientation functions describing the drawn state of the polymer are smaller than those corresponding to the rigid lattice situation. This is a very likely explanation when it is considered that the only possible way in which chain rotation can occur classically, without the hindrances imposed by the "gear-wheel" mechanism, described earlier is when the material is just below the melting point. Under these conditions the polymer is showing distinct signs of shrinkage and distortion since it is supported in an

unconstrained state on the shaft of the NMR probe. The orientation functions derived for the rigid lattice case are not applicable under these conditions.

Coherent classical rotation is not possible at temperatures lower than about 60°C because even if thermal lattice expansion is taken into account the resulting increase in the separation of the polyethylene chains is still insufficient to allow unimpeded rotation of the chains. Classical rotation must, therefore, be a pre-melting phenomenon associated with an almost liquid-like state of the polymer as exhibited by the narrowing of the absorption line shown in fig. 4.

4.2.2. Comparison of Experimental Results with a Chain Oscillation Model

It would appear intuitively reasonable that if chain oscillations are to occur at all they would precede coherent chain rotation. This, in fact, appears to be the case for temperatures above about − 40°C. It can be seen in fig. 6 that the curve corresponding to the variation of second moment with temperature for $\gamma = 90°$ meets the curve for $\gamma = 0°$ at − 100°C and only diverges again at − 40°C where the $\gamma = 90°$ curve is rapidly decreasing.

These results suggest that for temperatures above − 40°C the chains are undergoing classical oscillation about the *c*-axis, the effect of which will be intermediate between the rigid lattice situation and complete classical rotation. Andrew [7] showed that the primary effect of chain oscillation is to decrease the second moment at $\gamma = 90°$ more than at 0°. In addition the rapid decrease in the second moment in the range − 40°C upwards will be partly due to the increasing number of chains oscillating and also to lattice expansion, which will enable the amplitude of oscillation to increase.

4.2.3. Comparison of Experimental Results with a Chain Twisting Model

A feature exhibited by low density polyethylene is the continuous decrease in second moment at all angles over the complete temperature range. The curve for $\gamma = 90°$ falls below that for $\gamma = 0°$ at temperatures above − 40°C where we suggest chain oscillation is occurring. The initial low temperature decrease does not occur in linear polyethylene, and must therefore be associated with the presence of branch points.

It is of considerable interest that the second moment versus orientation curves for temperatures of − 100 and − 40°C shown in fig. 7, closely resemble the form of the curve for the anisotropy of the intramolecular rigid lattice second moment shown in fig. 8. A feature

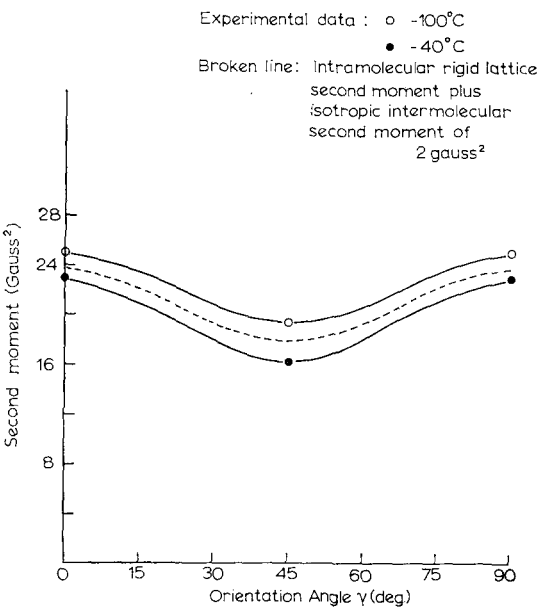

Figure 8 Comparison of intramolecular second moment anisotropy plus isotropic intermolecular interaction with experimental data obtained at temperatures of − 100 and − 40°C.

characteristic of the rigid lattice curve, shown in fig. 7, is the larger value of second moment for $\gamma = 90°$ than at $\gamma = 0°$. This is due to the effect of the intermolecular interactions which for a rigid lattice are highly anisotropic.

The symmetry of the curves for − 100 and − 40°C suggest that either (i) these intermolecular interactions are being averaged out and that the decrease in second moment from − 196 to − 40°C must be accounted for by intermolecular interactions, or (ii) intramolecular averaging must be occurring parallel to the chain axis to account for the decrease in the second moment at $\alpha = 0°$.

Let us first consider that the chains twist through a small angle perpendicular to the chain axis (see for example [8]) The chains could be regarded as held fixed at the folds at the lamella surfaces and thermally activated chain twisting could then occur in which successive CH_2 segments move through some angle θ with

respect to their neighbours. It is also reasonable to assume that the maximum angle of twist occurring at the centre of the chain length is created by successive segments moving through equal angles with respect to the previous segment.

In practice only small angles of twist are likely to occur, since any twist must be generated by simultaneous rotation about two C-C bonds in the planar zig-zag chain configuration of polyethylene, and large angles of twist will in any case not be possible, due to the large Van der Waals' interactions between chains.

The effect of the twist on the second moment parallel to the chain will now be discussed. As the chain twists it is expected that the proton interactions will decrease since the interproton distances will increase slightly. An effect of this type occurs in polytetrafluoroethylene in which a small deviation from the planar trans-configuration must occur due to Van der Waals interactions.

The actual calculation of the anisotropy of the second moment for various angles of chain twist can be carried out either by assuming a two-site model of the type described by Hoffman *et al* [8] or by assuming a particular form for energy function versus angle of twist.

The two site model, although perhaps not physically reasonable serves to provide us with an estimate of the effect of twist on the second moment. The calculation is carried out by calculating the expression:

$$\left\{\frac{3\cos^2\beta_{jk}-1}{r_{jk}^3}\right\}$$

in the distorted and non-distorted configuration' averaging and squaring the result to give the second moment.

It is easy to obtain an upper estimate of the effect of chain twisting on the second moment by calculating the rigid lattice second moment in the distorted state because the second moment should be very sensitive to small angles of twist. In fact, because of the inverse sixth power dependence of the second moment, it only requires a 10% increase in the interproton distances parallel to the chain to halve the intramolecular second moment. Qualitatively at least, this would appear to be a very hopeful mechanism in reducing the second moment at $\gamma = 0°$.

Computer calculations were accordingly carried out of the variation of the intramolecular rigid lattice second moment as a function of orientation angle for various angles of twist, the angle of twist being the angle between two successive monomer units. The results are shown in fig. 9. In fact the very small changes in the anisotropy with increasing angle of twist extends to much larger angles of twist than are shown in

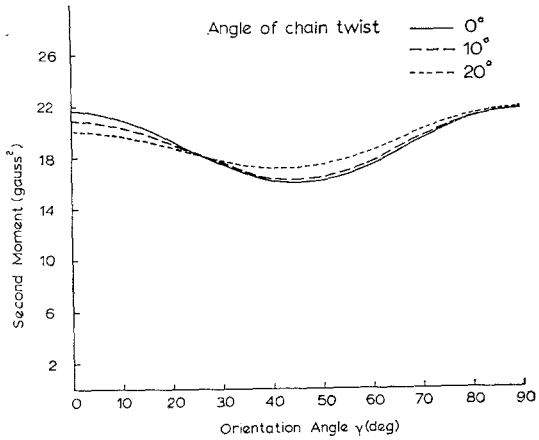

Figure 9 Intramolecular rigid lattice second moment versus orientation angle γ for various angles of chain twist for cold drawn low density polyethylene – draw ratio 3.7.

fig. 9, but this is not physically realistic. Of course it is necessary to emphasise once again that the curves in fig. 9 are an upper estimate of the anisotropy change with twist and that by computing

$$\left\{\frac{3\cos^2\beta_{jk}-1}{r_{jk}^3}\right\}$$

and invoking a specific analytic function to define the energy barrier for chain twisting, one can expect the invariance of the anisotropy with angle of twist to be even more marked.

These results lead to the conclusion that even if chain twisting is occurring, the observed anisotropy of the second moment with the orientation angle γ cannot be entirely due to this mechanism. It therefore seems most probable that the reduction in the second moment parallel to the chain direction is due to the averaging of the intermolecular interactions by neighbouring chains sliding past each other. We might expect that the effect of the Van der Waals' forces would be much less in this situation than in the corresponding case of chain twisting, where both large intra- and intermolecular interactions must be overcome.

4.2.4. Comparison of Experimental Results with a Chain Sliding Model

The intermolecular interactions for chain sliding will probably average to about the same value as for the calculation we carried out for rotating chains, that is, we can assume an intermolecular second moment ~ 1 to 2 gauss^2 and that it is approximately isotropic. If we add an isotropic contribution of 2 gauss^2 to the intramolecular rigid lattice curve we find that:

at $\gamma = 0°$ second moment ~ 24 gauss^2
$\gamma = 45°$,, ,, ~ 18 ,,
$\gamma = 90°$,, ,, ~ 24 ,,

These results are compared with the experimental curves corresponding to temperatures of − 100 and − 40°C in fig. 8 and we find that a very close fit is obtained at a temperature of − 70°C.

Comparison with the dynamic mechanical data (e.g. [5]) suggests that the molecular motion which we are invoking to explain the intermediate temperature NMR results must relate to the γ-relaxation, which occurs at − 120°C at a frequency ~ 10^2 Hz. Both low density and high density polyethylene show γ relaxation processes, and in both cases the relaxation appears to be a composite process involving at least one distinct relaxation for the crystalline and amorphous regions of the polymer respectively [8]. In this paper we have also analysed the changes in the broad component of the NMR signal only. The chain sliding process which we propose to explain the reduction in the intermolecular interactions, therefore provides a molecular interpretation of the crystalline γ relaxation process in low density polyethylene. Our data for NMR in low density polyethylene differs from that of Olf and Peterlin [1] for high density polyethylene, in that we observe large changes in second moment in the temperature range − 196°C to room temperature, whereas only small changes were observed in high density polyethylene. We therefore conclude that the γ relaxation processes in low density polyethylene include a chain sliding process which does not occur in the high density polymer. A possible process would be the γ_c process proposed by Hoffman *et al* [8] who envisage that an individual molecular chain rotates through 180° and is simultaneously translated along its axis.

The γ-relaxation is also attributed by many workers, e.g. Willbourn [11], to segmental motion of − CH_2 sequences in the amorphous regions. This mobility would give rise to the narrow component of the NMR signal as has been concluded by several investigators.

Irrespective of the detailed mechanism of chain sliding that occurs, it is clear that in the closely packed polyethylene lattice some occasional disorder, possibly due to branch points, is needed to provide space for *c*-axis chain translations at these low temperatures.This is in agreement with Hoffman *et al* [8] who suggest that the γ_c relaxation is dependent on the presence of defects and highly perfect crystals should show a practically negligible γ_c effect.

It should be mentioned that if the Hoffman mechanism operates under these conditions as distinct from a straightforward chain diffusion, the potential energy minima at the end points of the rotation of the chain must be very narrow, so that chains spend most of their time at either one or other of these minima and a negligible time in between. Thus we are visualising the case of 2-fold tunnelling, with delta function potential energy wells at ϕ and $\phi + \pi$. If the analytic function describing the energy barrier is of some other form, the resulting intramolecular interactions will not be those corresponding to the rigid lattice state but will be slightly reduced.

An exact quantitative evaluation of the effects of the Hoffman mechanism on the NMR second moment is difficult, due to lack of information on the specific eigen functions corresponding to a rigid rotator moving in a 2-fold potential. It can be shown that classical averaging of the angle ϕ during rotation is only valid for 3-fold potentials or higher and it is only in these cases that $\overline{\cos^2\phi} = \frac{1}{2}$ for complete rotation. For 2-fold potentials it can be shown that this average requires information concerning the eigen functions corresponding to the particular energy barrier.

5. Conclusions

The reduction in second moment of the broad component at intermediate temperatures can be attributed to a decrease in the intermolecular interactions by a chain sliding process. This process provides a molecular interpretation of a γ relaxation process in low density polyethylene.

As the temperature increases, chain oscillation occurs which finally leads to coherent classical rotation of the chains about the chain axes at temperatures close to the melting point of the polymer.

Acknowledgements

The authors are very grateful to Mr J. F. Munden for assisting in the experimental measurements and to their colleagues in the H. H. Wills Physics Laboratory, University of Bristol, for many useful discussions.

In this investigation we had occasion to recalculate the lattice sums and noted an error in one of these as previously reported. We are grateful to Professor E. R. Andrew for confirmation of this point.

Appendix

Effect of motion on the intramolecular second moment using spherical harmonic analysis

The Van Vleck equation for the second moment may also be written:

$$\langle \Delta H^2 \rangle = \frac{4G}{N} \sum_{j>k} r_{jk}^{-6} P_2^2(\cos \beta_{jk})$$

where $P_2(\cos \beta_{jk})$ is the second Legendre polynomial.

As before we must first express $P_2(\cos \beta_{jk})$ in terms of the intermediate angles θ_{jk}, ϕ_{jk}, δ and ϕ_δ defined in fig. 1. We can do this by applying the Legendre addition theorem:

$$P_2(\cos \beta_{jk}) = \frac{4\pi}{5} \sum_{m=-2}^{2} Y_{2m}^*(\theta_{jk}, \phi_{jk})\, Y_{2m}(\delta, \phi_\delta)$$

and the Y's are spherical harmonics defined by:

$$Y_{1m}(\theta, \phi) = \left[\frac{4\pi}{(2l+1)} \frac{(l+m)!}{(l-m)!}\right]^{-\frac{1}{2}} P_1^m(\cos \theta)\, e^{im\phi}$$

and $P_1^m(\cos \theta)$ are the associated Legendre functions.

Now we require

$$\langle P_2(\cos \beta_{jk}) \rangle_{\phi_{jk}} = \frac{4\pi}{5} \left\langle \sum_{m=-2}^{2} Y_{2m}^*(\theta_{jk}, \phi_{jk})\, Y_{2m}(\delta, \phi_\delta) \right\rangle_{\phi_{jk}}$$

and this must be averaged over 2π. Considering only the ϕ dependent part of $Y_{1m}(\theta, \phi)$ it can be seen that this average will take the form:

$$\frac{1}{2\pi} \int_0^{2\pi} e^{im(\phi_\delta - \phi_{jk})}\, d(\phi_\delta - \phi_{jk}) = \frac{1}{2\pi} \left[\frac{e^{im(\phi_\delta - \phi_{jk})}}{im}\right]_0^{2\pi}$$

$= 0$ unless $m = 0$.

Hence

$$\langle P_2(\cos \beta_{jk}) \rangle_{\phi_{jk}} = \frac{4\pi}{5} Y_{20}^*(\theta_{jk}, \phi_{jk})\, Y_{20}(\delta, \phi_\delta) = P_2(\cos \theta_{jk}) \,.\, P_2(\cos \delta) \,.$$

We now square this result and relate δ to the intermediate angles Δ, ϕ_Δ, γ and ϕ_γ and finally average ϕ_Δ over the range 0 to 2π to account for the transverse isotropy of the c-axes of the units of structure.

Therefore,

$$[\langle P_2(\cos \beta_{jk}) \rangle_{\phi_{jk}}]^2 = P_2^2(\cos \theta_{jk})\, P_2^2(\cos \delta) = P_2^2(\cos \theta_{jk}) \sum_l a_l P_l(\cos \delta)$$

where $P_2^2(\cos \delta)$ has been expanded as a series of Legendre polynomials so that the addition theorem can be applied to each term of the series. If the addition theorem is applied to each term of the series and an appropriate average over ϕ_Δ taken, we find:

$$\langle [\langle P_2(\cos \beta_{jk}) \rangle_{\phi_{jk}}]^2 \rangle_{\phi_\Delta} = P_2^2(\cos \theta_{jk}) \sum_l a_l P_l(\cos \gamma)\, \overline{P_l(\cos \Delta)}$$

Thus we may substitute this into the Van Vleck equation and get:

$$\langle \Delta H^2 \rangle = \frac{4G}{N} S \sum_l a_l P_l(\cos \gamma)\, \overline{P_l(\cos \Delta)}$$

where S is a lattice sum defined by

$$S = \sum_{j>k} r_{jk}^{-6} P_2^2(\cos \theta_{jk})$$

and if $P_2^2(\cos \theta_{jk})$ is expanded as above we may write:

$$S = \sum_{j>k} r_{jk}^{-6} \sum_l a_l P_l(\cos \theta_{jk})$$

References

1. H. G. OLF and A. PETERLIN, *J. Appl. Phys.* **35** (1964) 3108-14.
2. *Idem, Kolloid Z.* **215** (1967) 97-111.
3. V. J. MCBRIERTY and I. M. WARD, *Brit. J. Appl. Phys.* **1** (1968) 1529-42.
4. J. H. VAN VLECK, *Phys. Rev.* **74** (1948) 1168-83.
5. N. G. MCCRUM, B. E. READ, and G. WILLIAMS "Anelastic and dielectric effects in polymeric solids" (Wiley, 1967), p. 353.
6. C. P. SLICHTER, "Principles of magnetic resonance" (Harper and Row, New York 1963) p. 62.
7. E. R. ANDREW, *J. Chem. Phys.* **18** (1950) 607-18.
8. J. D. HOFFMAN, G. WILLIAMS, and E. PASSAGLIA, *J. Polymer Sci.* **C14** (1966) 173-235.
9. D. W. MCCALL and W. P. SLICHTER, *J. Polymer Sci.* **26** (1957) 171-86.

10. J. A. SAUER and A. E. WOODWARD, *Rev. Mod. Phys.* **32** (1960) 88-101.

11. A. H. WILLBOURN, *Trans. Faraday Soc.* **54** (1958) 717-29.

Received 25 July 1970 and accepted 9 March 1971.

Since this paper was submitted for publication an NMR study of molecular motion in oriented long chain alkanes by Olf and Peterlin has appeared in print (*J. Polymer Sci.* A(2) **8,** (1970), 753). Further T_2 measurements on low density polyethylene have also been reported by McCall and Falcone (*Trans. Faraday Soc.* **66,** (1970), 262.